Chapter 4: Results and discussion

41. The single QD detection and fluorescence decay time

Due to the optical diffraction limit, it is a challenge to distinguish the emission from a single QD from the QD cluster. Due to the unique features of single QD, like fluorescence intermittency, the measurement on the optical properties of single QD could be possible. It is crucial to optically isolate QD from each other for the single QD detection. To optically isolate QD, after the capping of CdSe colloidal QD by ZnS shell, we injected 0.03mL of QD drop, which has QD concentration of 10^{-9}M, on a 18×18mm^2 glass cover slip, and then was uniformed by the spin cast at 6000rpm. The average distance between the QD is about 1μm, which is larger than the laser spot of 0.3μm in diameter. The cover slip was loaded onto the holder which is mounted on the microscopic manual stage. The laser beam was focused by the oil objective, which positions below the stage and can be moved by the piezo-controller. The fluorescence of the single quantum dots was collected with the same microscope objective, separated from the scattered laser light by dichroic mirror and guided to the SPAD through a 50μm diameter pinhole. The fluorescence image and atomic force microscope image are shown in Figure 4.1.1 (a) and (b), respectively.

An important indication for existence of one single QD is the fluorescence blinking. The streaks on the fluorescence image arise from the discrete turning on/off single QD's emission. This can be also illustrated in fluorescence image lateral profile in Figure 4.1.1 (c) (d). We set the intensity threshold (10 counts/ms) above the background noise (5counts/ms) to define the emissive (on) and non-emissive (off) state. For single QD, its MCS trace shows the obviously on-off abrupt transition,

instead of the continuous one (see Figure 4.1.1 (e) (f)). Besides, Efros proposed that the intensity for each on or off state is definite [18]. However, the intensity fluctuates with time for each emissive state in our experiment. This extended problem is attributed to the quantum yield fluctuation with time, i.e. there exists a non-constant non-radiative decay rate, which varies with time. In addition, there exists a weak emission in the off-state, it might come from the autofluorescence from the glass coverslip or the other background noise.

To study the fluctuation of lifetime, we obtained a lifetime distribution profile for every single QD (see Figure 4.1.2 (a)).By comparing the respective fluorescence decay curves for an individual single QD at different fluorescence intensity region, while lowers the count rate threshold, it can be clearly seen that the lifetime decay curve represent a non-linear trajectory at log scale (see Figure 4.1.2 (b)), and the lifetime distribution broadens and shifts to shorter lifetime region (see Figure 4.1.3 (a)). For setting low intensity threshold condition, the low intensity burst would be counted. This refers to the decay curve is composed of a significant number of low intensity burst, which more related to additional non-radiative channel relaxation, so a non-linear decay curve will be performed. The decay rate observed in single QDs time-resolved experiment is the sum of the radiative and non-radiative decay rate ($k_{obs}=k_{fl}+k_{nr}$), i.e., the observed decay time can be express as $\tau_{obs}=\tau_{fl} / (\tau_{fl}/\tau_{non}+1)$. For setting low intensity threshold condition, a lower intensity burst, which has more non-radiative photons, has large τ_{non} variation, so a lifetime distribution will be broadening. Also, the existence of factor τ_{non} will lead to the lifetime distribution shift to lower lifetime region. In order to avoid the non-radiative induced quantum yield fluctuation, we collected the data by setting the count rate threshold at high intensity region. The data collocating manner refer to the other research for single QDs

time-resolved experiment [19, 20].

Furthermore, to distinguish the degree of lifetime distribution, the fluorescence decay curve was fitted by Kohlrausch-William-Watts (KWW) function, commonly known as stretching exponential function:

$$I(t) = I_0 \cdot e^{-(t/\tau_{1/e})^\beta} \qquad (2)$$

where $\tau_{1/e}$ is the average radiative lifetime while the fluorescence curve decays to $1/e$. The stretching exponent β ($0 < \beta \leq 1$) denotes the lifetime distribution broadening rate. The statistic of β histogram for high and low intensity region is shown in Figure 4.13 (b). As the mention above, the measured fluorescence decay curve consists of radiative and non-radiative process decay. If we set the low intensity threshold from the MCS trace, which implies that more non-radiative burst counted (higher k_{nr}), the fluorescence decay curve would show multi exponential decay, and by fitting KWW function in this condition, we would get a small β value. The small β value represents the high distribution rate, i.e. a broadened lifetime distribution. In this case, the non radiative decay rate k_{nr} which fluctuates with time becomes considered, thus we can not get the exact radiative lifetime in this way. In the opposite, if we chose the higher region from MCS trace, the ratio of radiative to non-radiative photons are highly increased in each burst, and we get the β approach to unity (for ideal single exponential decay, β exactly equals to one). In this case, the radiative lifetime is a constant and does not fluctuate with time.
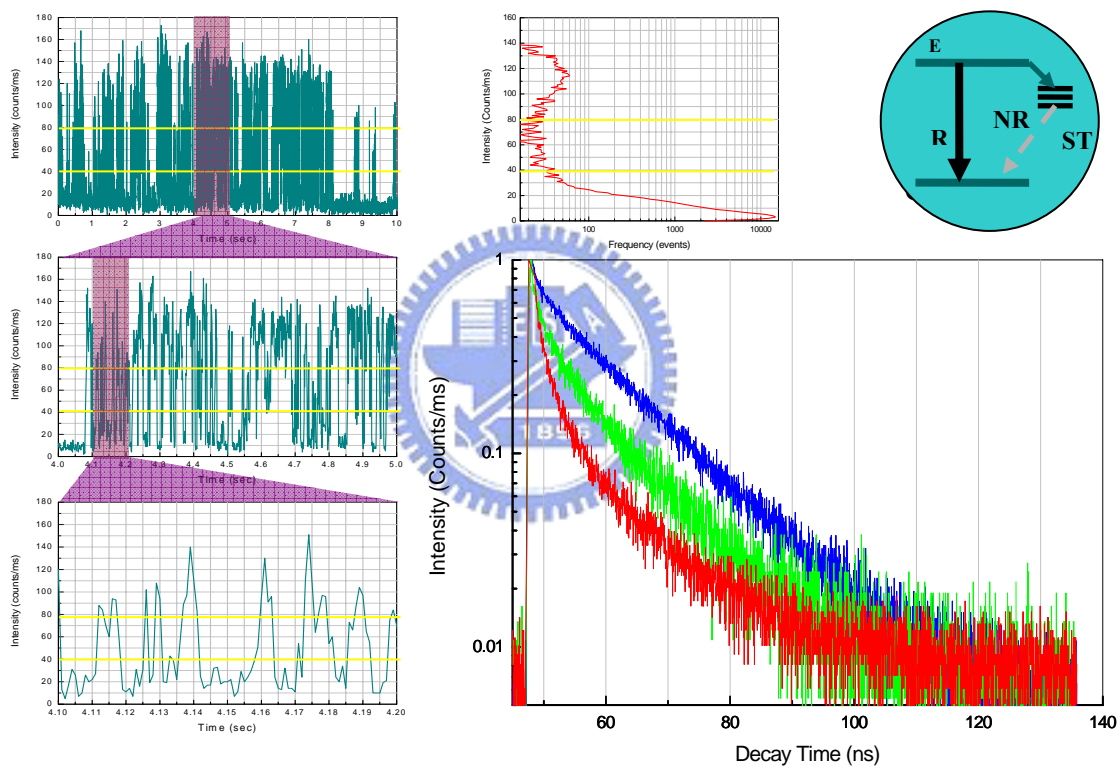
(a)

(b)

(c)

(d)

(e)

(f)
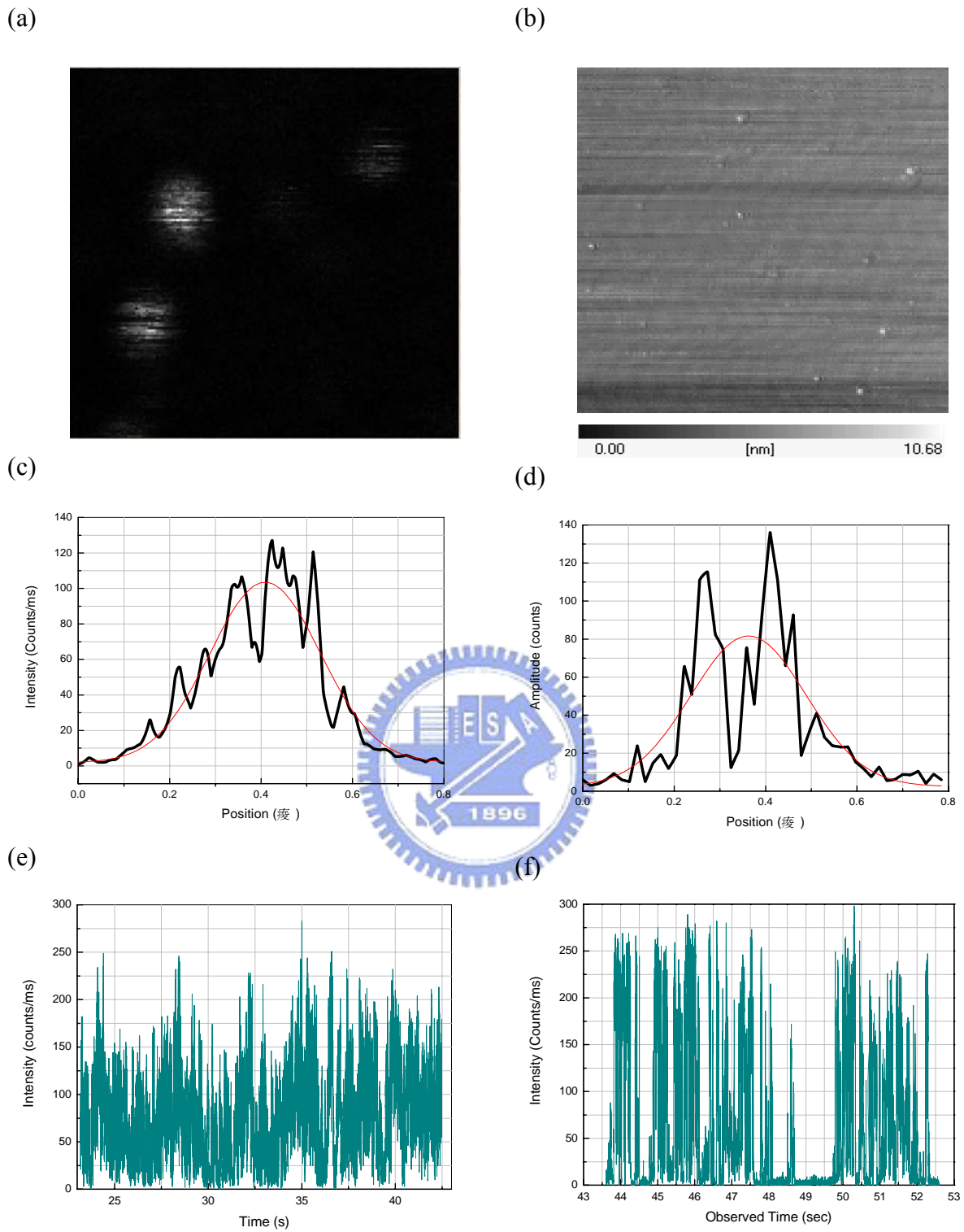
Figure 4.1.1 (a) Fluorescence image and (b) AFM image of colloidal CdSe QDs. Fluorescence image lateral profile of (c) multi QDs and (d) single QDs. Time trace of (e) multi QDs and (f) single QDs.
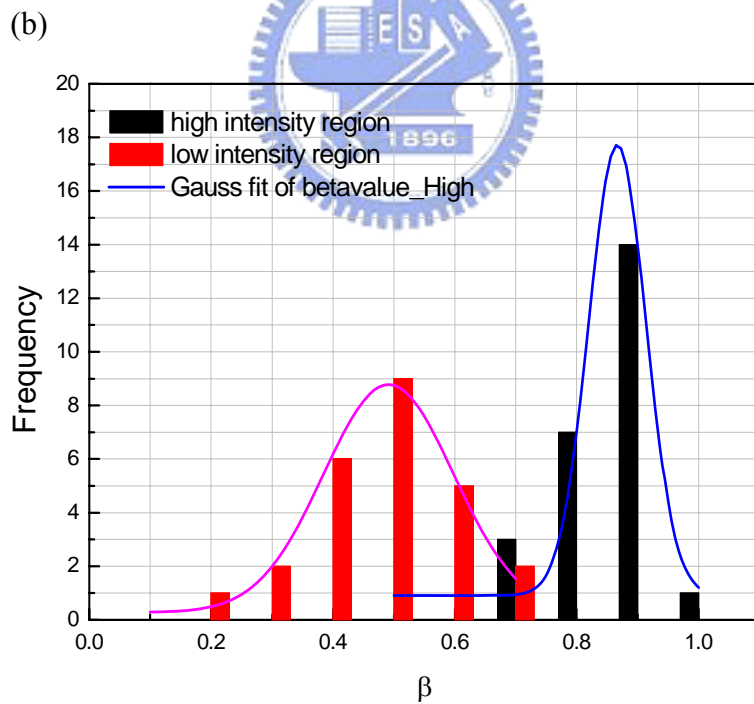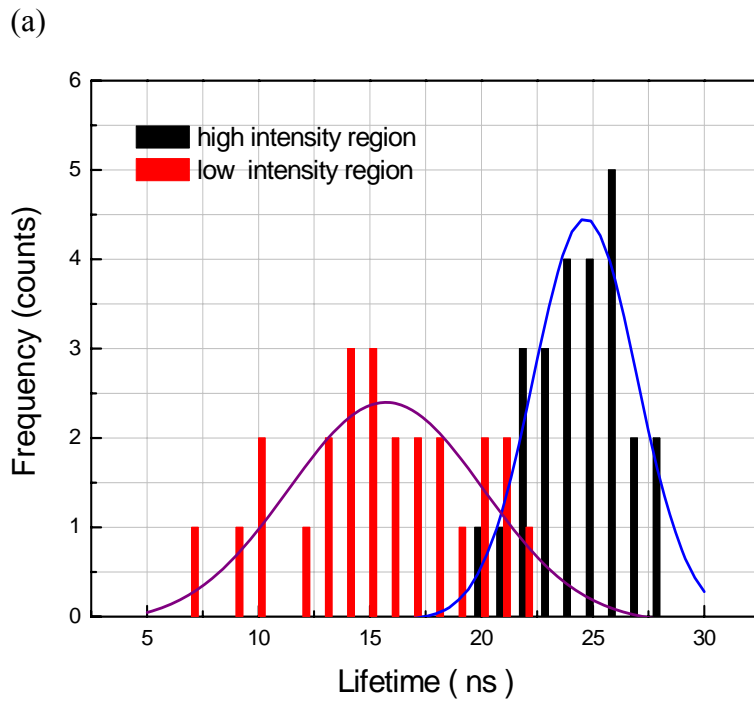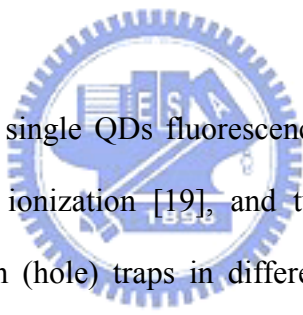
(a)
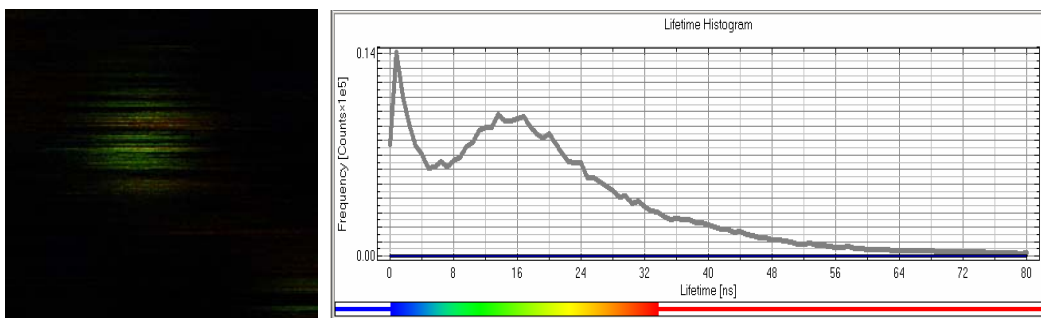
(b)

Figure 4.1.2   (a) Lifetime distribution histogram of single QDs, and (b) Fluorescence decay curve of single quantum dot

(a)

(b)

Figure 4.1.3   (a) Lifetime distribution histogram, and (b) β distribution histogram of single quantum dot for high and low intensity region of time trace.

4.2 Power dependent intermittency of CdSe/ZnS quantum dot

In this section, we study the excitation power dependent intermittency of CdSe/ZnS single QDs. Fluorescence intermittency refers to the abrupt transition of period of bright and dark state with time trajectory. While a single QD is excited by laser, it generates an electron-hole pair in the core of CdSe, subsequently the electron-hole relaxes to the band edge by phonon relaxation. When the excited electron-hole recombines, it emits a photon, and then the duration of emissive ("bright" or "on") state occurs. However, if the electron (hole) is trapped by surface state, or surrounding trapping level, the emissive state will be stopped and then turned to the non-emissive ("dark" or "off") state, until the trapped electron (hole) is back to the core of QD.

It was proposed that the single QDs fluorescence intermittence is attributed to Auger process [18], thermal ionization [19], and tunneling effect [20]. Different process may lead the electron (hole) traps in different location (see Figure 4.2.1). Auger process may lead electron (hole) trap far away from the QD, and the thermal effect may lead to the electron (hole) trap in the QD surface dangling bond. Thus, for the far trapped electron (hole), it is hard to return to the core of CdSe, i.e. the non-emissive time interval will be extended. For CdSe/ZnS QDs, the high band offset can block the electron (hole) ionized by thermal effect. Thus, the thermal effect induced ionization can be ignored.

By different ionized mechanism, the behavior of fluorescence intermittence is related to the ionized electron (hole) location. In Figure 4.2.2, the left part of figure reveals the dramatic blinking behavior which comes from the thermal effect. Via the thermal effect, the electron (hole) was injected and then trapped at the core/shell

interface easily, and also returned to the core for the same way, so the fast on-off transition rate could be obtained. The right part of figure shows the Auger process induced dark state, a longer off-time interval is observed. Particularly, the middle one shows that if the electron and hole are both trapped in the surrounding, the subsequent generated electron (hole) is hard to eject to surrounding due to Coulomb blockade. However, this situation is rare to happen.

Here, we carried out the power dependence of CdSe/ZnS single QDs to observe the variation of fluorescence intermittency. Figure 4.2.3 shows the examples of typical MCS trace and count rate histogram by excitation power dependence, from 550 emission line CdSe/ZnS single QDs. The average value of excitation power from top to bottom are 0.1, 1, 10μW respectively. The MCS traces with 1 second scale show that the blinking frequency dramatically enhances while excitation power increases, and the corresponding count rate histograms show that the photon count intensity shifts to higher region but has significant reduction of burst event. Besides, the intensity below 10 counts/ms is regard as the background noise. Three examples of on and off time histograms with different excitation power are shown in Figure 4.2.4. , and we use the inversed power law (eq. (1)) for fitting equation. The value of *m* indicates the transition rate of on to off (off to on) for on-time (off-time) histogram. For on-time histogram, we got the m value are 1.42, 1.54, 1.89, the corresponding average on-time interval are 18 ms, 10 ms, 6 ms by the power law. The on-time interval reduces while the excitation power enhances. Also, the off-time histogram analysis has been carried out by the same way. The *m* values are between 1 and 2, and the average off-time interval is in millisecond order, however, there is no tendency observed while the excitation power enhanced.

In the conclusion of Figure 4.2.3 and Figure 4.2.4, it is clearly seen that the fluorescence intermittency for lowest power one has the longest on-time interval, but reduced dramatically with excitation power enhancement. This result can be attributed to that the QD ionization is dominated by the Auger process. The Auger process indicates that if the QD generates two electron-hole pairs at same time, one of electron-hole pair will transfer their energy (about 2.1eV for CdSe) to the third particle (electron or hole), thus, the third particle has the ability to jump out of the high band offset (about 0.7 eV for CdSe/ZnS). Auger process happens in picoseconed order, faster than radiative lifetime (nanosecond order), so there is no photon emission at two electron-hole pair condition. At high excitation power condition, the probability of the biexciton state generation becomes large, and this result in the electron (hole) in QD ejects to the deep localized level of surrounding efficiently.

Furthermore, the on-off time histogram provides evidence of blinking behavior. Interestingly, the probability distribution of the length of on (off) time interval is followed by the power law statistics. The most probable explanation for the inverse power law behavior of the off state is the existence of multiple ionization states and consequently a distribution of recombination rates. Furthermore, in order to explain the inversed power-law behavior of on time distribution, Kuno et al [21] proposed that electron tunneling events are considered. Indeed, according to our experiment result, both on and off time histograms obey the power-law distribution for all cases. However, the off-time interval is found to be independent on excitation power.

Another spectacular phenomenon of single QDs is the variation of lifetime with excitation power dependence. Figure 4.2.5 shows the examples of lifetime distribution profile with different excitation power for CdSe/ZnS single QDs. The excitation

power from top to bottom is 0.1μW, 0.4μW, 0.7μW, and 1μW respectively, and the corresponding average lifetime is 20 ns , 17ns, 16 ns, and 12 ns. The lifetime below 4 ns may come from the glass coverslip autofluorescence. The similar result has also been demonstrated in the other experiments [22, 23]. Figure 4.2.6 shows the corresponding lifetime-intensity correlation histogram, the coloring scheme denote the histogramming frequency. While increasing the excitation power, the lifetime distribution will be narrowing and shift to the lower region. Furthermore, the burst event of higher intensity region is dramatically enhanced than the lower one, this indicates that at high excitation power the fluorescence emission is dominated by radiative process. Thus, we can make sure that the emission photon for the reduction of lifetime distribution by excitation power is really from the radiative process, instead of the non-radiative process.
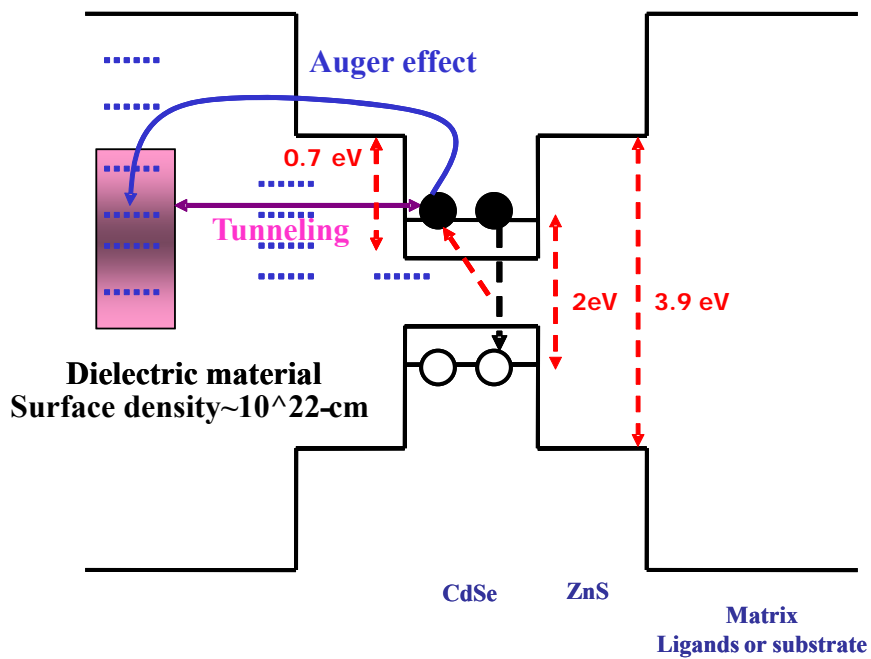
Figure 4.2.1 Ionized process of single QDs. Three different ways, Auger, thermal, and tunneling effect may occur.
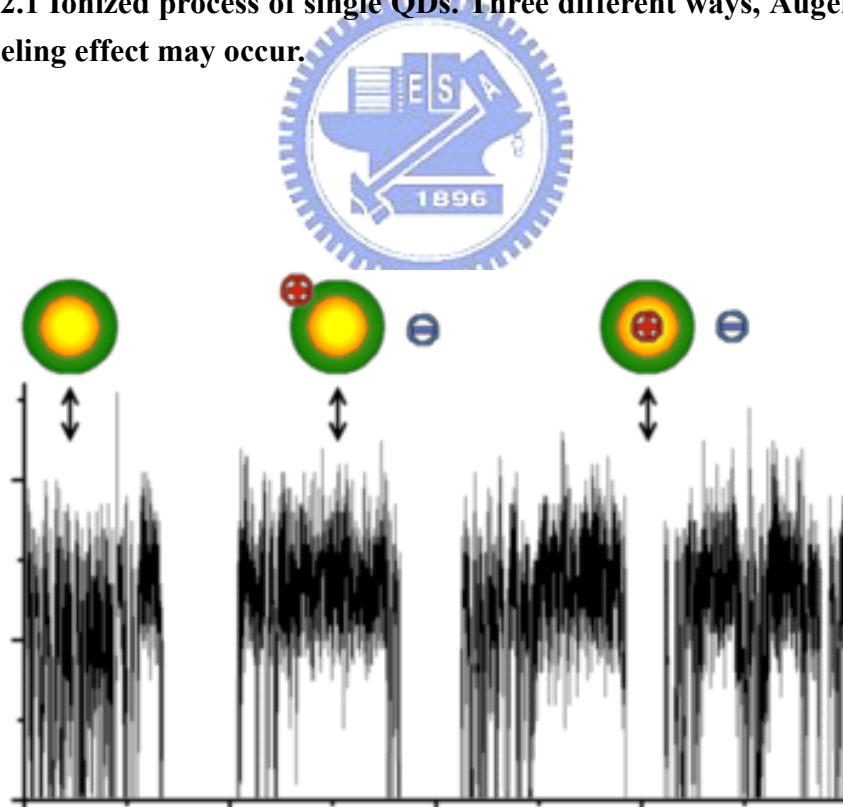
Figure 4.2.2 Fluorescence time trace of single QDs. Three different types, blinking, on time, off time, may be observed.
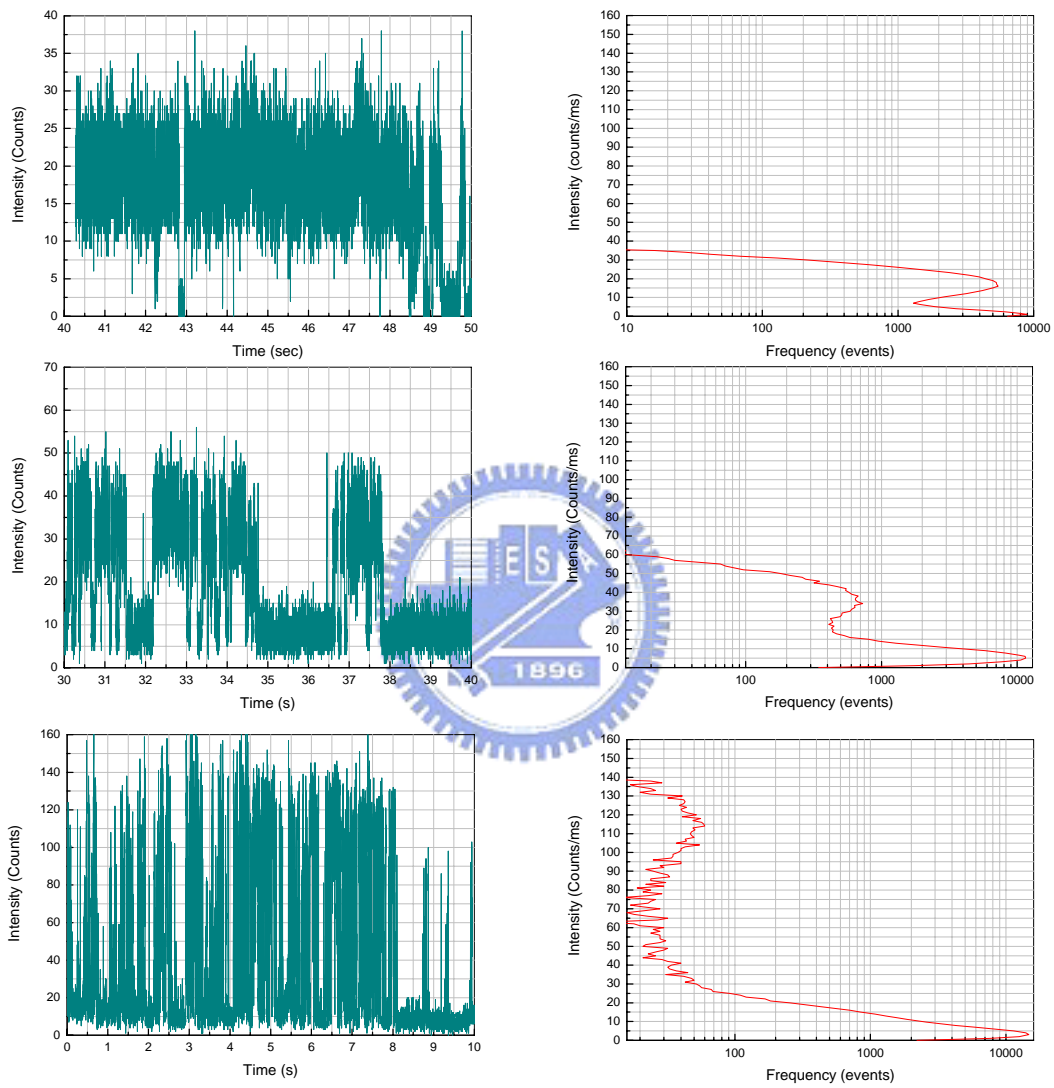
Figure 4.2.3   Time traces with 01 μW, 1 μW, and 10 μW excitation power from top to bottom respectively.

Figure 4.2.4   On time (left) and off time (right) histogram with $0.1\,\mu\mathrm{W}$, $1\,\mu\mathrm{W}$, and $10\,\mu\mathrm{W}$ excitation power from top to bottom respectively. The on (off) time histograms are fitted by a power law $N(\tau_{on/off}) = At^{-m}$
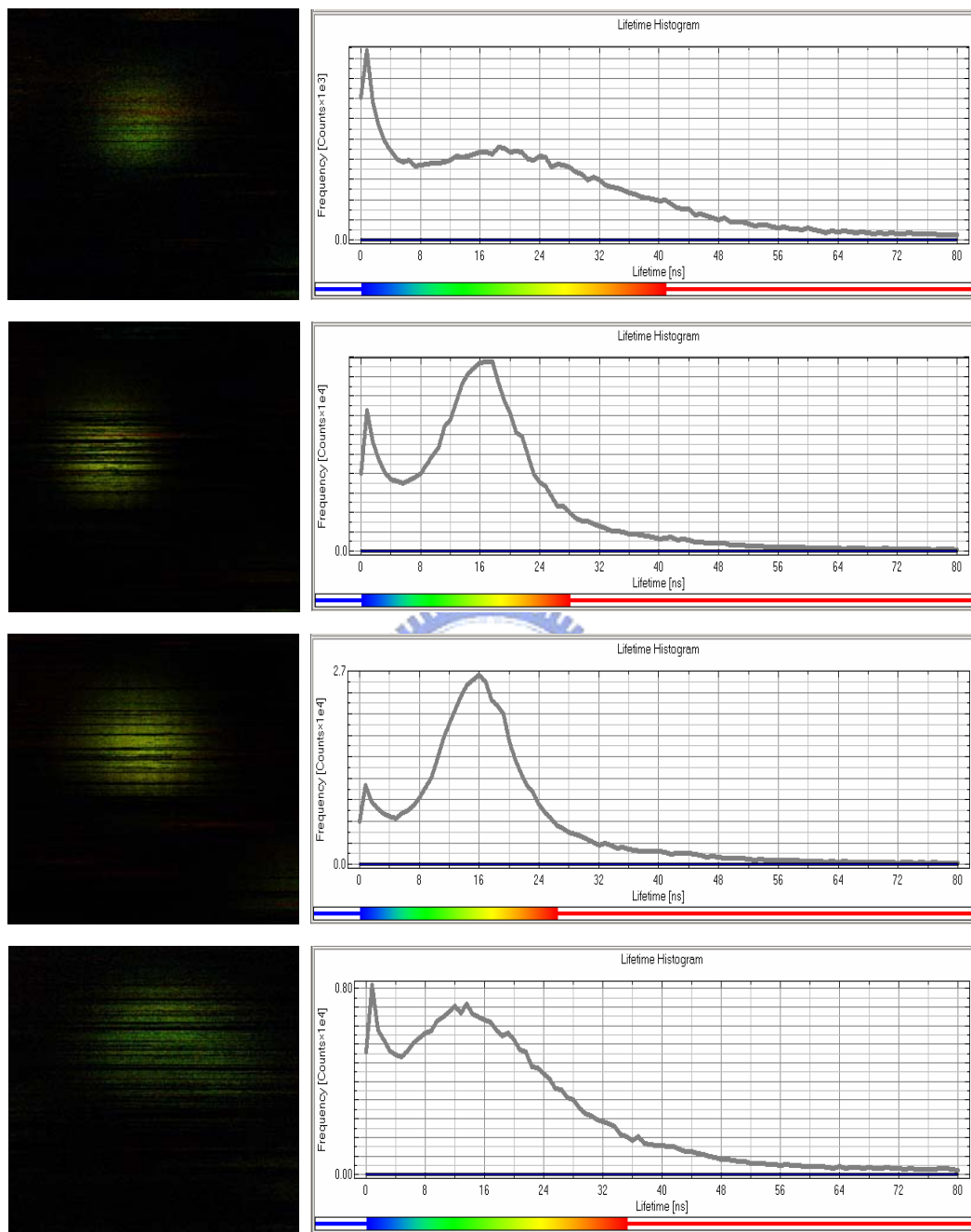
Figure 4.2.5 Lifetime distribution profile 0.1µW, 0.4µW, 0.7µW, and 1µW excitation power respectively.
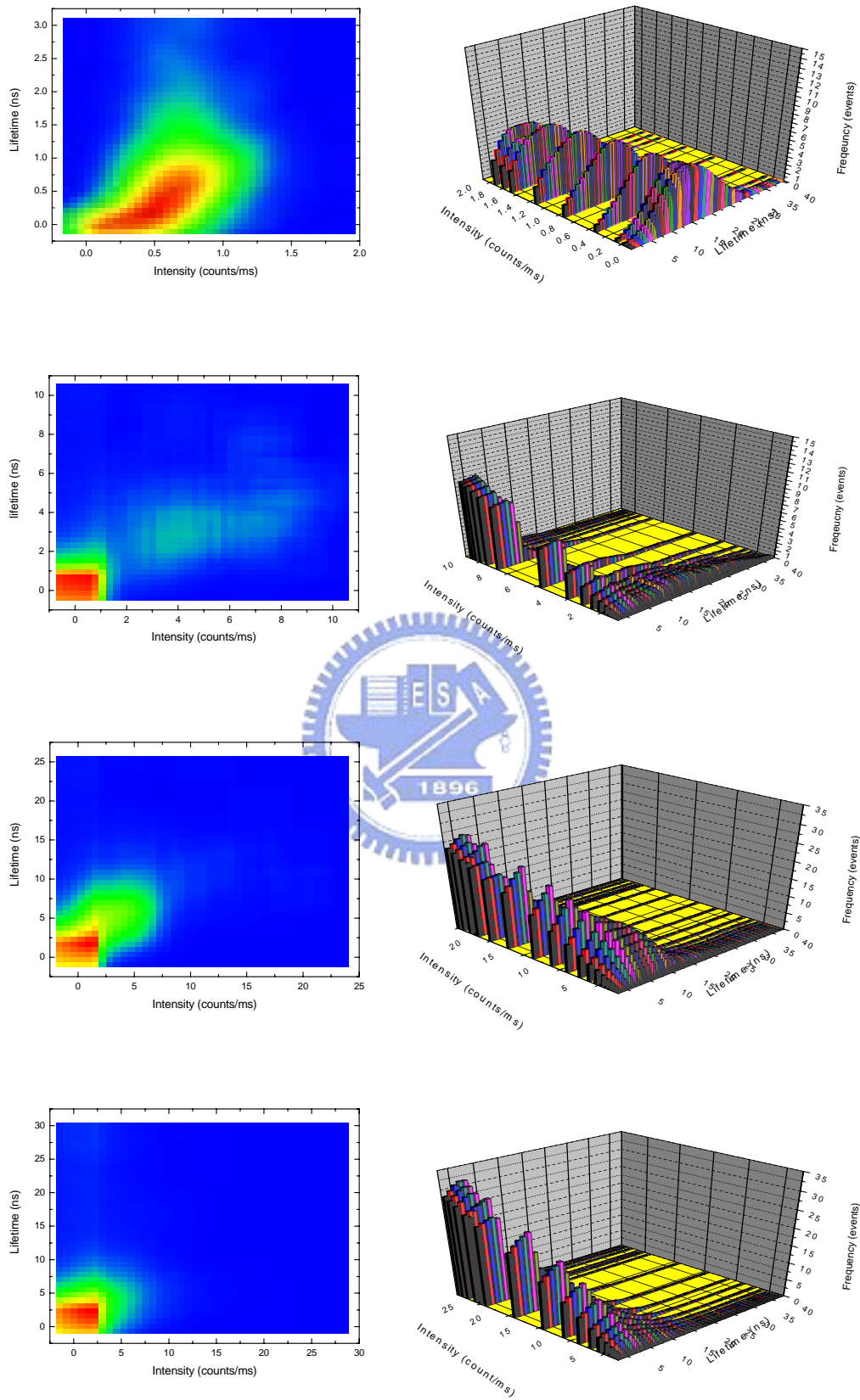
Figure 4.2.6 The lifetime-intensity correlation histogram for CdSe single QDs with 0.1μW, 0.4μW, 0.7μW, and 1μW respectively.

4.3 CdSe/ZnS quantum dot with metal surrounding

In this section we discuss the effect of insulating and conducting surrounding on the optical properties of single QDs. The bare glass substrate was replaced by the substrate which has Au nanoparticles. The absorption of Au nanoparticles with 13nm in diameter and the photoluminescence spectrum of CdSe/ZnS QDs are shown in Figure 4.3.1. The absorption peak of Au nanoparticles with 13nm in diameter is at 523nm, and the emission line of CdSe/ZnS QDs is at 540nm. The absorption of Au nanoparticles partially overlaps with the emission spectrum of CdSe/ZnS QDs. As a result, the plasmon of Au nanoparticle resonances with the CdSe/ZnS QD fluorescence is expected to occur.

Figure 4.3.2 shows the time trace of CdSe/ZnS QD on glass coverslip and Au nanoparticle coated glass coverslip respectively. It can be clearly seen that the Au nanoparticle mixed sample has intensity two-fold larger than the sample without Au nano-particles. Figure 4.3.3 shows the power dependent intensity. The intensity of QD mixed with Au nanoparticle is higher then that of QD without Au nano-particles. In both cases, the fluorescence intensity saturated at high power region. Figure 4.3.4 shows the corresponding burst size histogram, more burst events occurs for QD mixed with Au nanoparticle. The enhancement of QD mixed with Au nanoparticle might come from the plasmon resonance [24].

In Figure 4.3.5, the on (off)-time histogram of QD and QD with Au nanoparticle are fitted by inversed power law equation (eq. (1)), and the *m* values are 1.57 (1.45) and 1.19 (1.07) for CdSe/ZnS QD and CdSe/ZnS QD with Au nano-particle, respectively. A smaller *m* value of on (off) histogram for CdSe/ZnS with Au one indicates that the transition will be reduced when the Au nanoparticle is added. In

Figure 4.3.6, the obvious larger lifetime for QD with Au indicates that a remarkable

elimination of non-radiative process. Also, in Figure 4.3.7, it can be clearly seen that

the statistic of on-time interval as excitation power function diagram for QD with Au

nanoparticle has the significant larger on-time then of QD. Furthermore, in Figure

4.3.8, the statistic of blinking frequency as excitation power function diagram show

that the QD with Au nanoparticle has the lower blinking frequency then that of QD

for each power. The similar result has also been demonstrated by the other experiment

which use ITO glass for conducting surrounding [25]
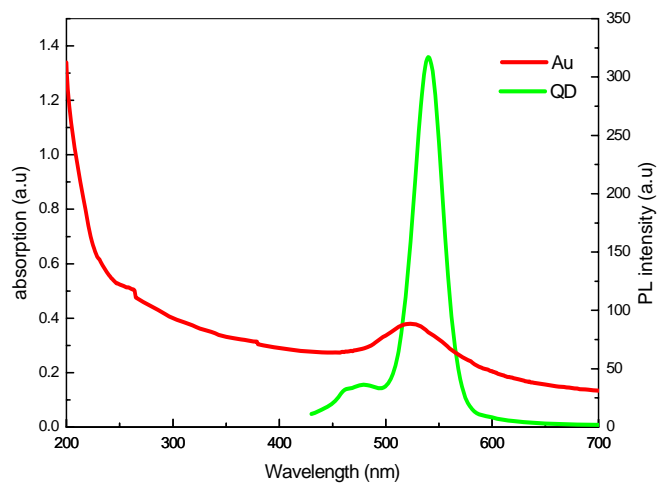
Figure 4.3.1   Photoluminescence of CdSe/ZnS QD (QD) and absorption of Au nanoparticle.

(a)

(b)
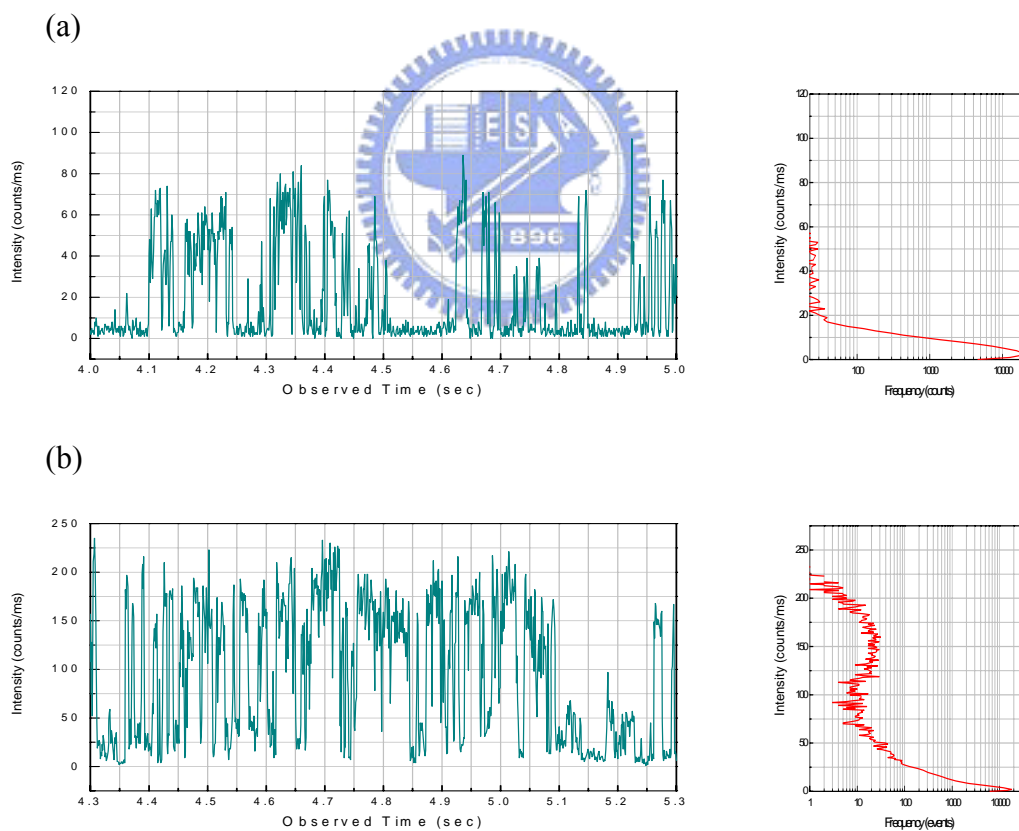
Figure 4.3.2   Time trace of CdSe/ZnS on (a) glass coverslip, and (b) Au nanoparticle coated glass coverslip.
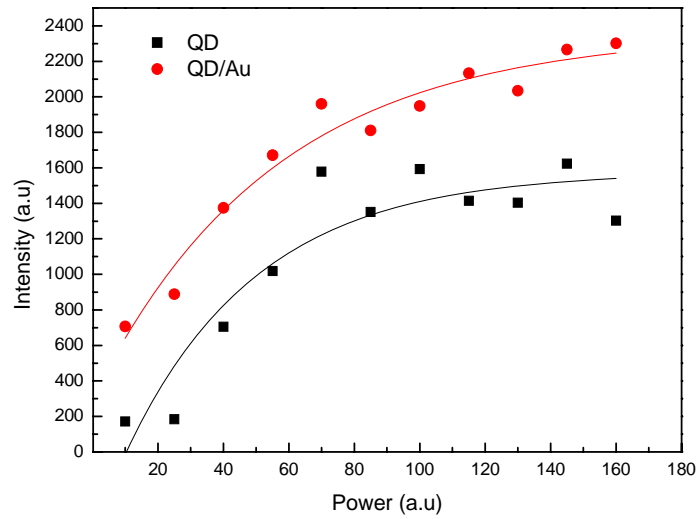
Figure 4.3.3   Power dependent fluorescence intensity of quantum dot (QD) and quantum dot with Au nanoparticle (QD/Au).

(a)   (b)
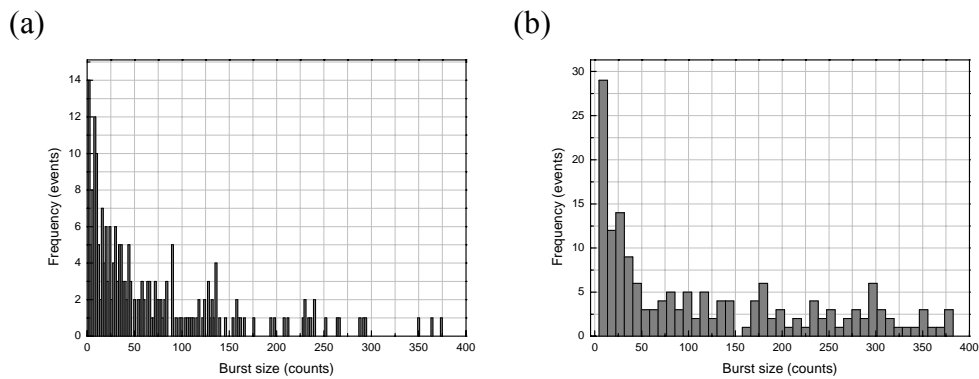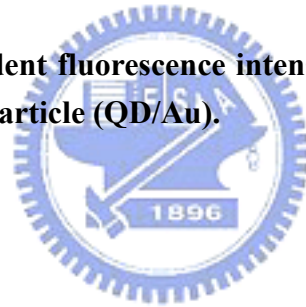
Figure 4.3.4   Burst size histogram of (a) CdSe/ZnS QD and (b) CdSe/ZnS with Au nanoparticle.

(a)
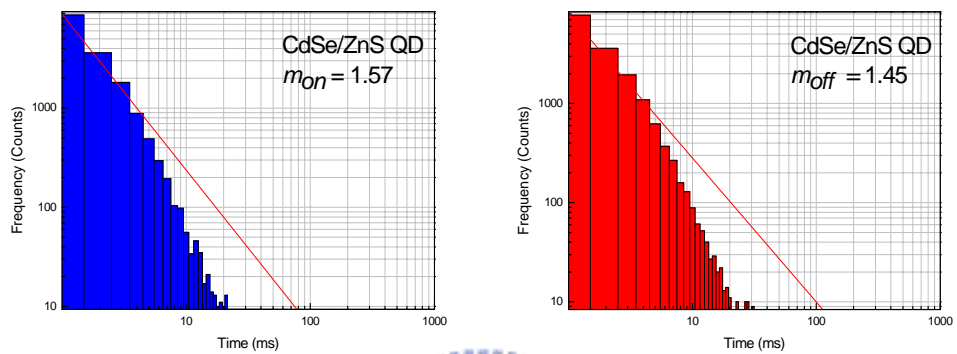
(b)
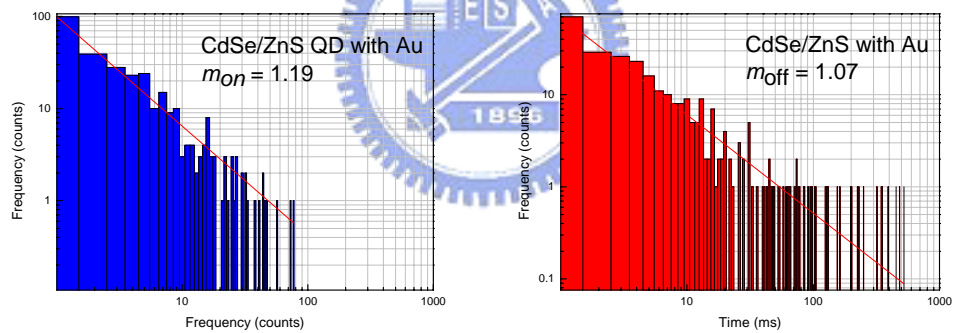
Figure 4.3.5   Power dependent on time (left) and off time (right) histogram of (a) CdSe/ZnS QD and (b) CdSe/ZnS with Au nanoparticle.
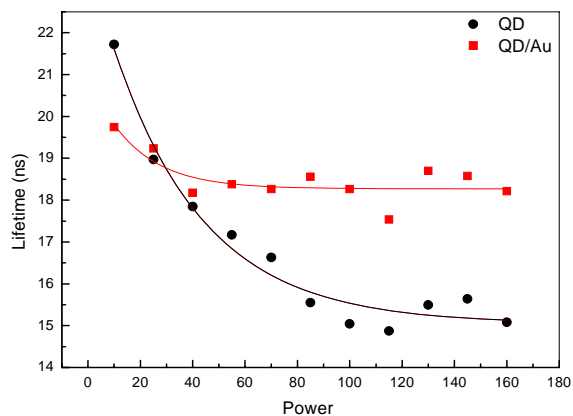
Figure 4.3.6   Power dependent lifetime of quantum dot (QD) and quantum dot with Au nanoparticle (QD/Au)
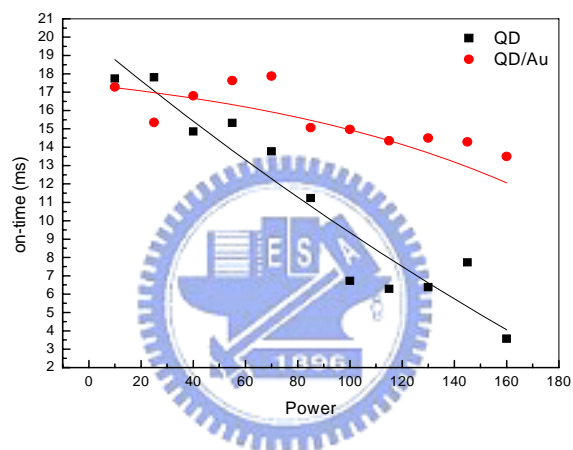
Figure 4.3.7   Power dependent on-time of quantum dot (QD) and quantum dot with Au nanoparticle (QD/Au)
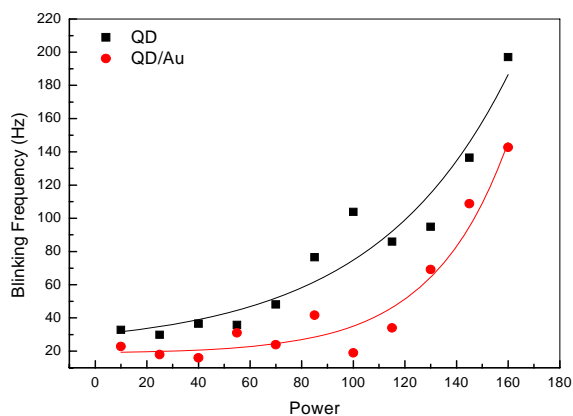
Figure 4.3.8   Power dependent blinking frequency of quantum dot (QD) and quantum dot with Au nanoparticle (QD/Au)

4.4 The size dependence of CdSe/ZnS quantum dot

Three kinds of CdSe/ZnS QDs samples of different sizes have been utilized in our experiment. The diameter of QD is 2nm, 3nm, and 6nm respectively. All CdSe nano-crystals were coated by 1 monolayer ZnS, and also soluble in chloroform. The photoluminescence spectra from CdSe/ZnS QDs clusters of different sizes were shown in Figure 2.1.1 (c). The emission lines are in the visible region (462nm (2.68eV) for blue, 564nm (2.29eV) for green, and 640nm (1.94eV) for red). The emission intensity has been normalized. The peak appears at 480nm on the green line shoulder may arise from the defect localization.

Figure 4.4.1 and Figure 4.4.2 shows the time trace and burst size histogram of single QDs with different sizes. It can be clearly seen that the green one has the highest intensity and more events of larger size burst, and the blue one is on the opposite. Figure 4.4.3 shows the on-off time histogram of single QDs with different sizes. By fitting the inversed power law for on (off) time histogram, we get the value m equals to 1.64 (1.30), 1.44 (1.29), 2.3 (1.05) respectively. For green light QDs, a smallest m_{on} indicates that on to off transition rate is lowest, and a higher m_{off} indicates that the off to on transition rate is higher. Thus, the green line QD emission is mainly on emissive state in the same time. In the opposite, for blue light QDs, a significant higher m_{on} and lower m_{off} indicates that it is mainly on non-emissive state. The red light QDs has lower m_{on} value and higher m_{off} then blue one, but higher the m_{on} value then green one. Thus, the average on-time interval of time trace for red line QDs is between green light and blue light QDs.

Figure 4.4.4 show that the single QDs comparison of lifetime with excitation power dependence. From the 0.1μW to 10 μW, the lifetime of green line QDs is from

22ns down to 16 ns, and the red line QDs is from 18ns down to 13ns in exponential decay. The blue line QDs is from 16ns down to10ns in linear decay. The green line QDs has the highest lifetime for single QDs is attributed to its longer emissive state and higher intensity for each emissive state. Figure 4.4.5 shows the on-time interval as a function of excitation power. From the 0.1μW to 10 μW , the on-time interval for the green line QDs is from 18ms to 5ms in linear decay, the red line QDs is from 12ms down to 6ms in exponential decay, and the blue line QDs is from 6ms down to 3ms in exponential decay. Figure 4.4.6 shows the blinking frequency as a function of excitation power, from the 0.1μW to 10 μW the blinking frequency for the green line QDs is from 30Hz increase to 200Hz, the red line QDs is from 20Hz increase to 80Hz, and the blue line is from 4Hz increase to 40Hz. Our results shows that the fluorescence intermittency is independent with QD size, and the lifetime might only correspond to the quantum efficiency of sample.

(a)

(b)

(c)
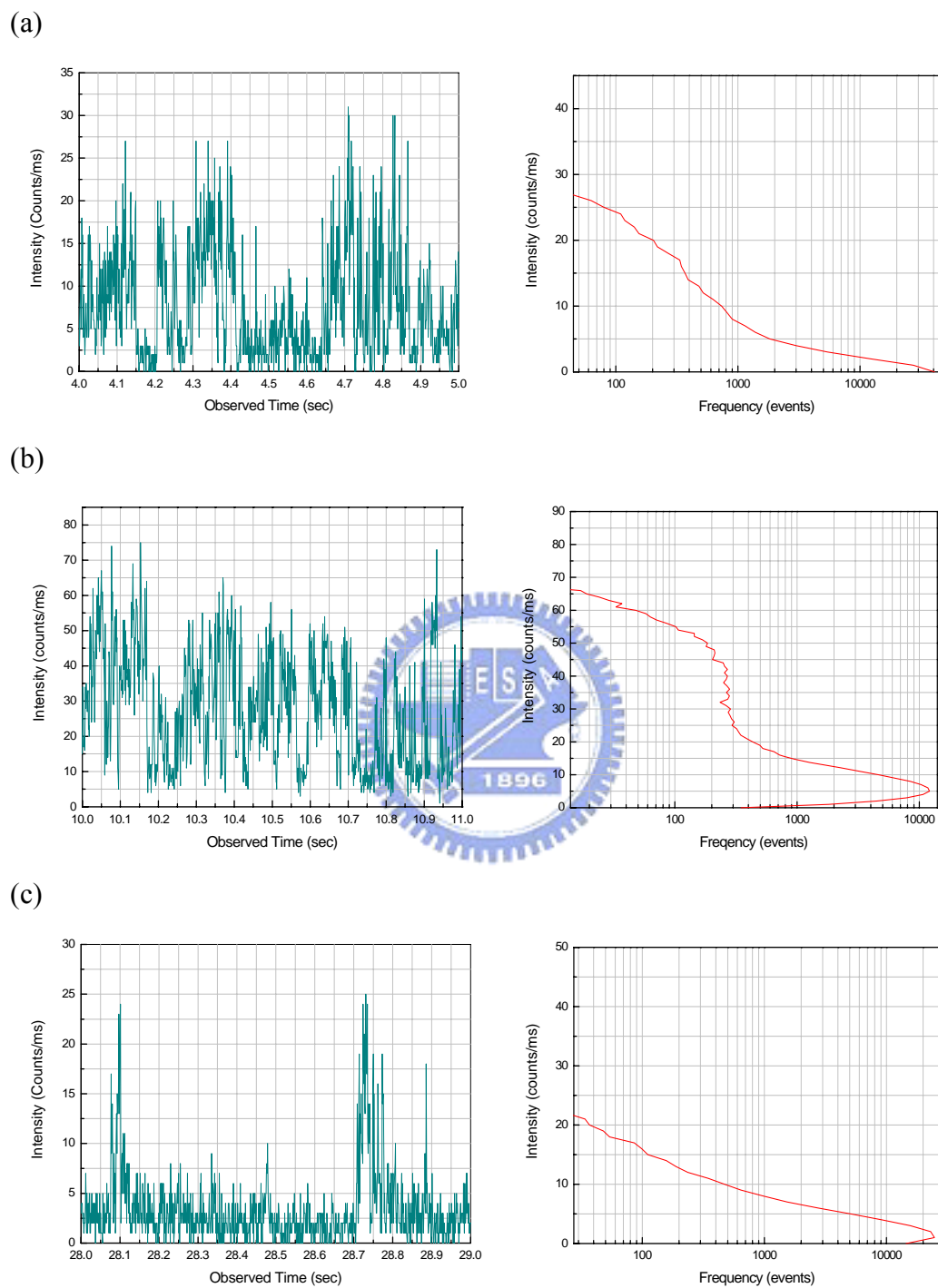
Figure 4.4.1   Time trace of single CdSe/ZnS QDs of (a) 6nm, (b) 3nm, and (c) 2nm in diameter.
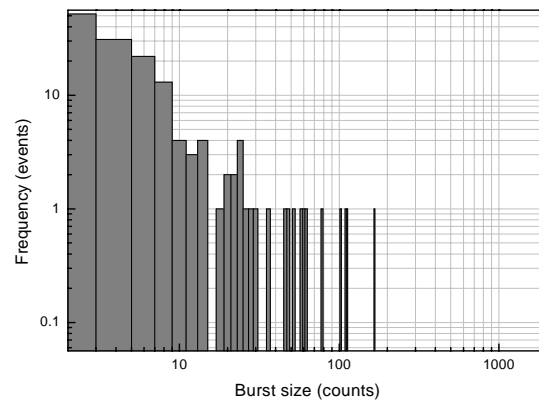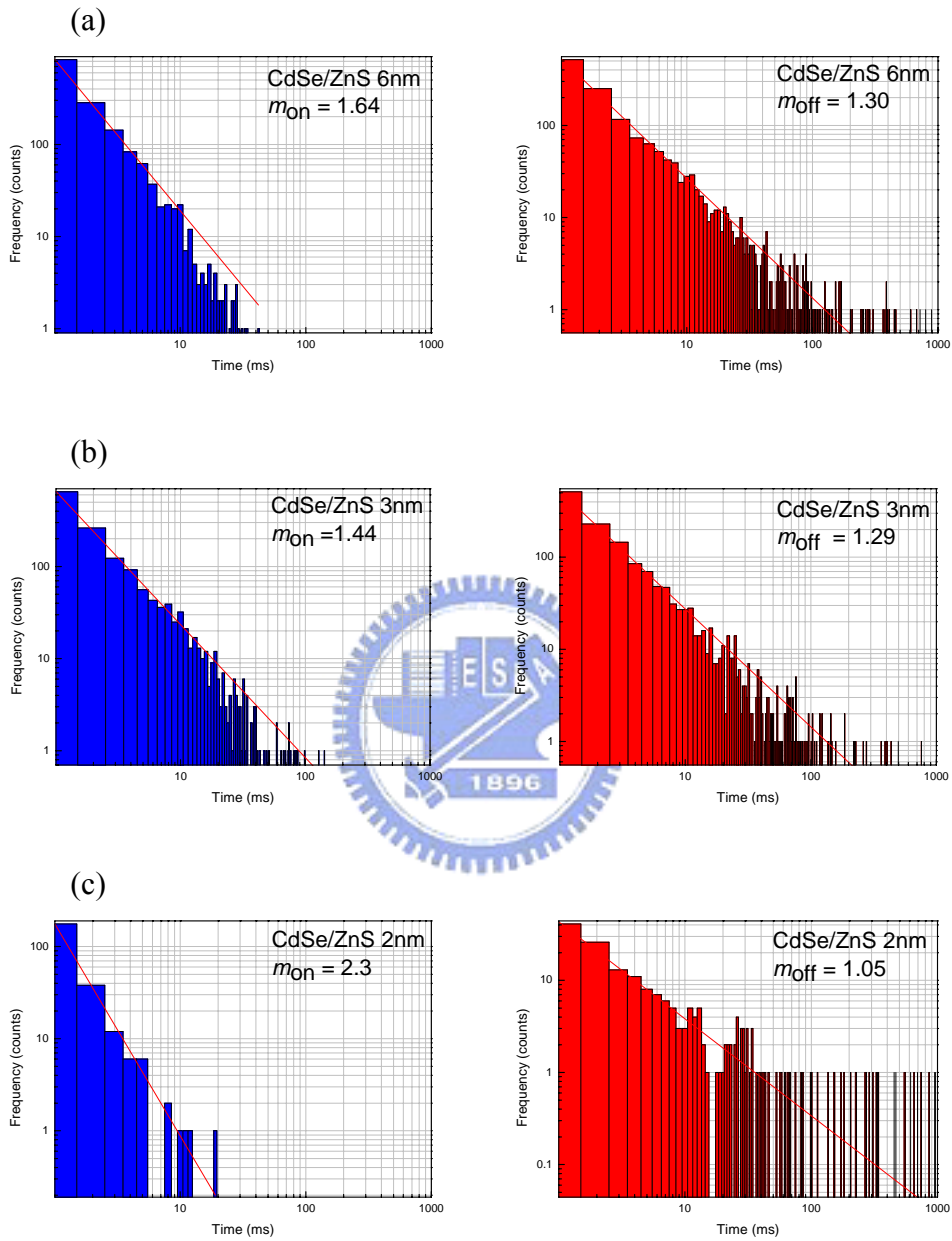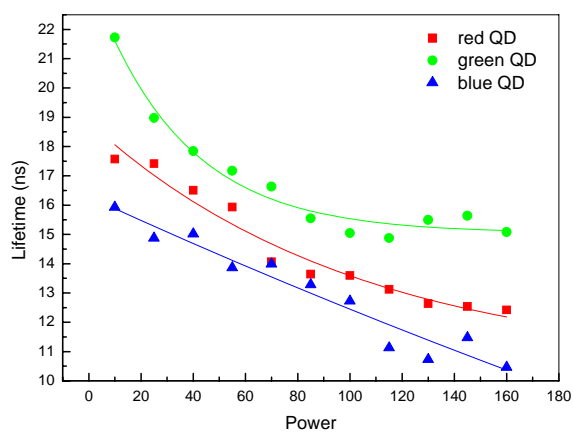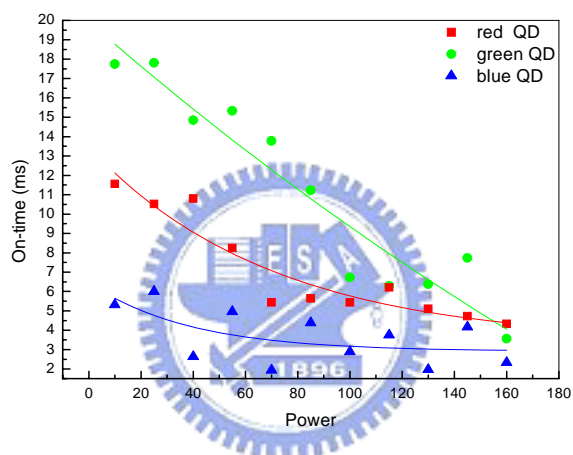
(a)
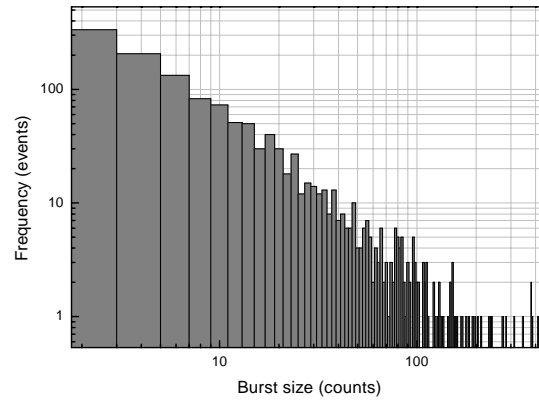
(b)
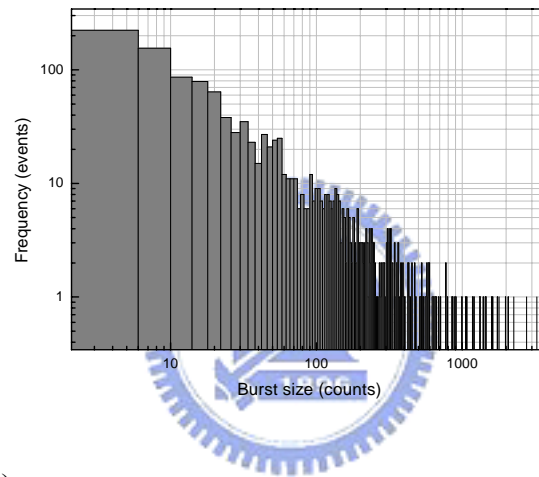
(c)

Figure 4.4.2   Burst size histogram of CdSe/ZnS QDs of (a) 6nm, (b) 3nm, and (c) 2nm in diameter.
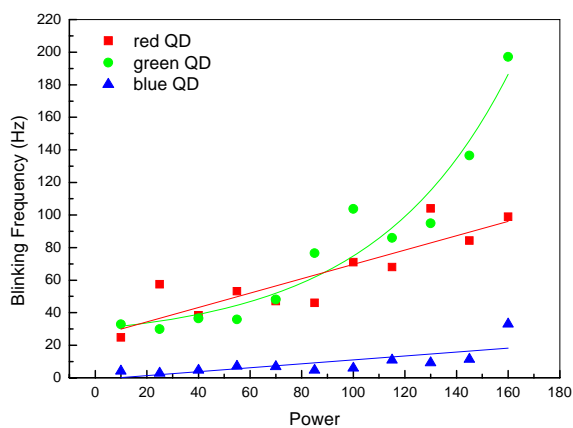
Figure 4.4.3   On-time (left) and off-time (right) histogram of single CdSe/ZnS QDs of (a) 6nm, (b) 3nm, and (c) 2nm in diameter.

Figure 4.4.4   Power dependent lifetime of quantum dot with different sizes.

Figure 4.4.5   Power dependent on-time of quantum dot with different sizes.

Figure 4.4.6   Power dependent blinking frequency of quantum dot with different sizes.

4.5 The ligand conjugation of CdSe (/ZnS) quantum dot

In this section, we compared the emission properties of CdSe Qds and CdSe/ZnS QDs with different kinds of surface ligand conjugations. Here, we replace the organic ligand by TOPO, TOPO-HDA (HDA added latter), TOPO-HDA-PA (PA added subsequently after the HDA), and TOPO-HAD,PA (HDA and PA added at the same time). The ligand molecular formula is listed in Table 2.1.1. The PL spectra of surface ligand conjugated CdSe and CdSe/ZnS QD clusters for green line are shown in Figure 4.5.1 and Figure 4.5.2, respectively. For CdSe nanocrystal series, the PL spectra shows that the emission line shifts to lower energy position for TOPO-HDA and TOPO-HDA-PA. It can be attributed the increase in effective size by the ligand conjugation of QD, this results in the wavefunction extension to wider boundary and also lowers its emission energy. However, the emission line of CdSe-TOPO-HAD,PA has blue shift which is different from the others. For the CdSe/ZnS QDs series, the emission line shows the red shift for TOPO-HDA and TOPO-HDA-PA ligand conjugation, but blue shift for TOPO-HAD,PA. Although, the ligand conjugation could increase its effective size, the higher ZnS barrier decreases the extension of wave-function dramatically. Therefore, the position of emission line will be affected slightly for the CdSe/ZnS QD case. In addition, comparing the intensity of CdSe and CdSe/ZnS QDs, the intensity of CdSe/ZnS series is 2.5 to 17.5 times larger than CdSe one.

In the view of single QDs, the time traces of CdSe and CdSe/ZnS QDs are shown in Figure 4.5.3 and Figure 4.5.4 respectively. It can be clearly seen that there are significant differences of on (off) time interval and blinking frequency, between CdSe and CdSe/ZnS QDs. For CdSe nanocrystal, the on-off abrupt transition is fast and thus lower on (off) time interval. For CdSe/ZnS QDs, the high band gap ZnS can prevent the electron (hole) ejected to the surrounding by Auger ionization, thus, a longer

on-time interval would be exist. In the opposite, the ejected electron (hole) would hardly return to the core of QDs either, so the off-time would also be longer. Figure 4.5.5 and Figure 4.5.6 show the on-off time histogram of CdSe and CdSe/ZnS, respectively. Fitting by inversed power law equation for the on histogram, we get the value m of CdSe QD series is higher then the CdSe/ZnS one. It indicates that higher on to off transition is for CdSe nanocrystal series. In Figure 4.5.7, the burst histogram shows that the CdSe/ZnS QD has broader burst size distribution, lower burst frequency, i.e. longer on-time interval and lower blinking frequency as mention above.

Figure 4.5.8 shows the radiative decay curves of CdSe and CdSe/ZnS, and all the average lifetimes are listed in Table 4.5.1, the lifetime of CdSe series are below 10 ns, which is lower then the CdSe/ZnS with 8 to 16 ns. The shorter lifetime for CdSe indicates that it has lower quantum efficiency then CdSe/ZnS. Furthermore, we use the stretch exponential function to fit the decay curve. The obtained value β implies the lifetime distribution rate, if β approach to unity, the lifetime distribution rate reduced. Thus, if the non-radiative process is reduced by the ligand conjugation with great surface passivation, this will result in lower lifetime distribution rate, i.e. β approach to unity. Here, for CdSe serious, the β are respectively equal to 0.8, 0.3, 0.5, and 0.5 for TOPO, TOPO-HDA, TOPO-HDA-PA, and TOPO-HDA, PA. The low β for HDA ligand conjugation might comes from the increase of the CdSe surface state, so broadening the lifetime distribution rate. However, for CdSe/ZnS serious, we get the β are equal to 0.7, 0.8, 0.9, and 0.6. One reason of the high β value is CdSe surface passivated by ZnS coating, another one is by the ligand conjugation. We got the TOPO-HDA-PA has the best surface passivation, but worst for TOPO-HDA, PA. All the physical parameters are listed in Table 4.5.1.
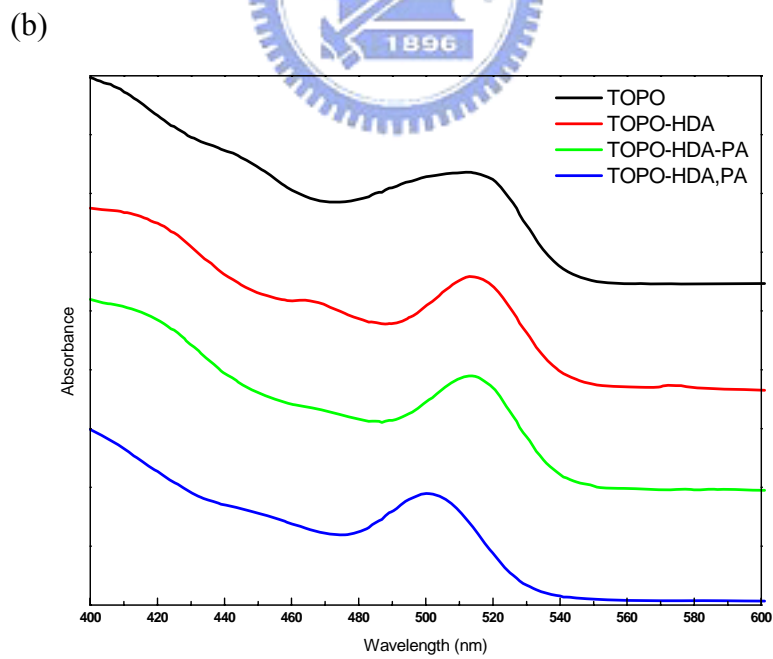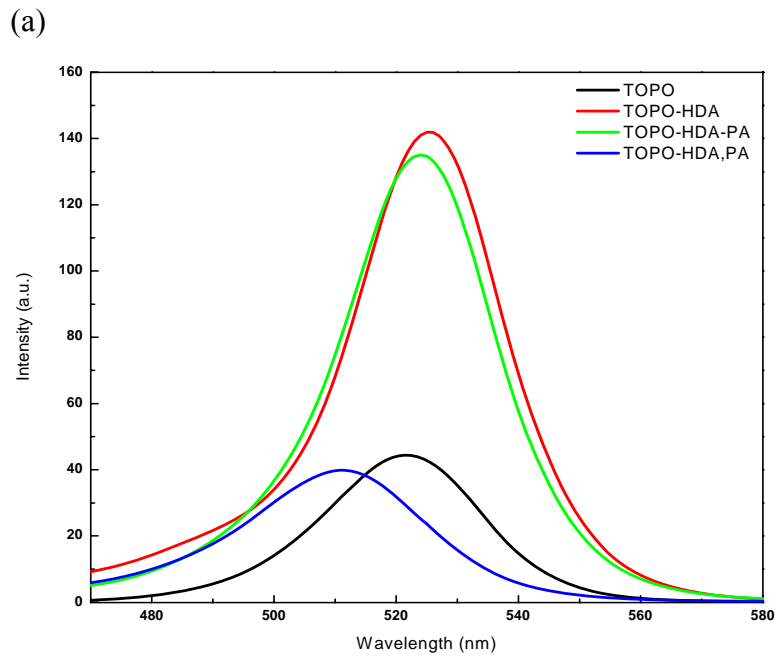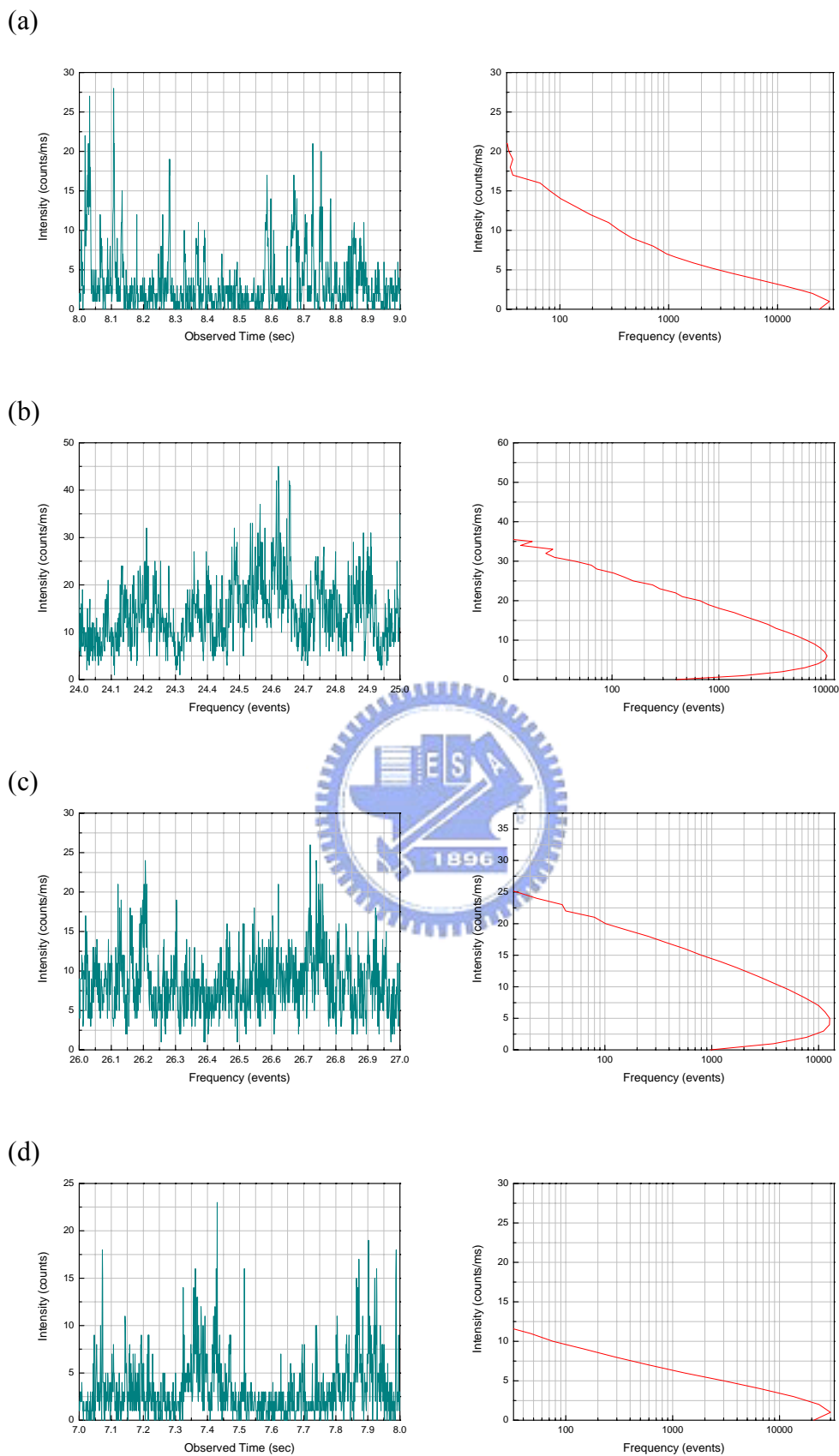
(a)
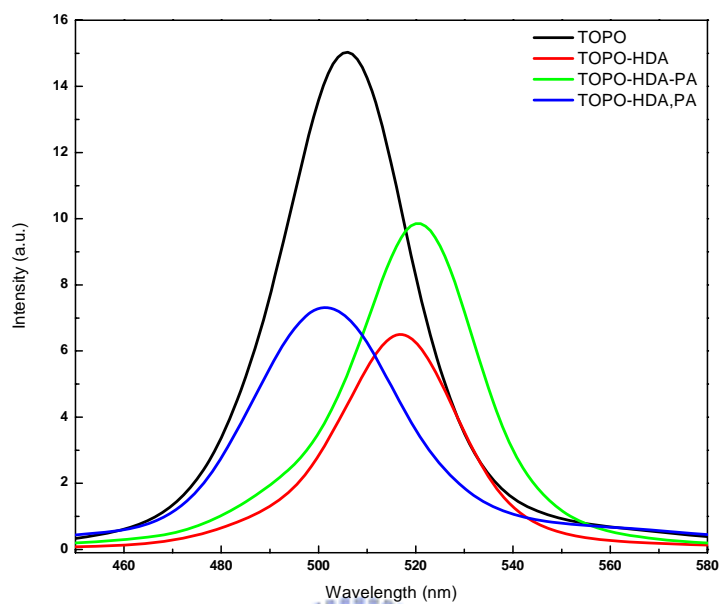
(b)
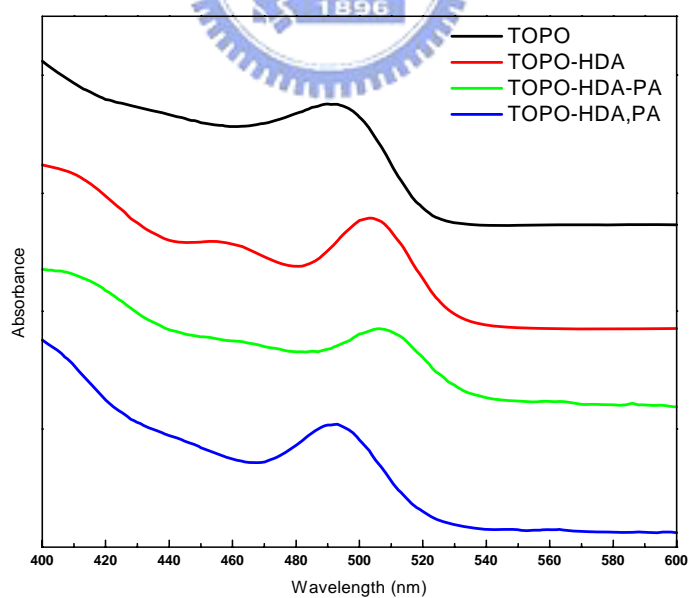
Figure 4.5.1   (a) PL and (b) absorption spectra of surface-ligand CdSe nanocrystal of 3nm in diameter.
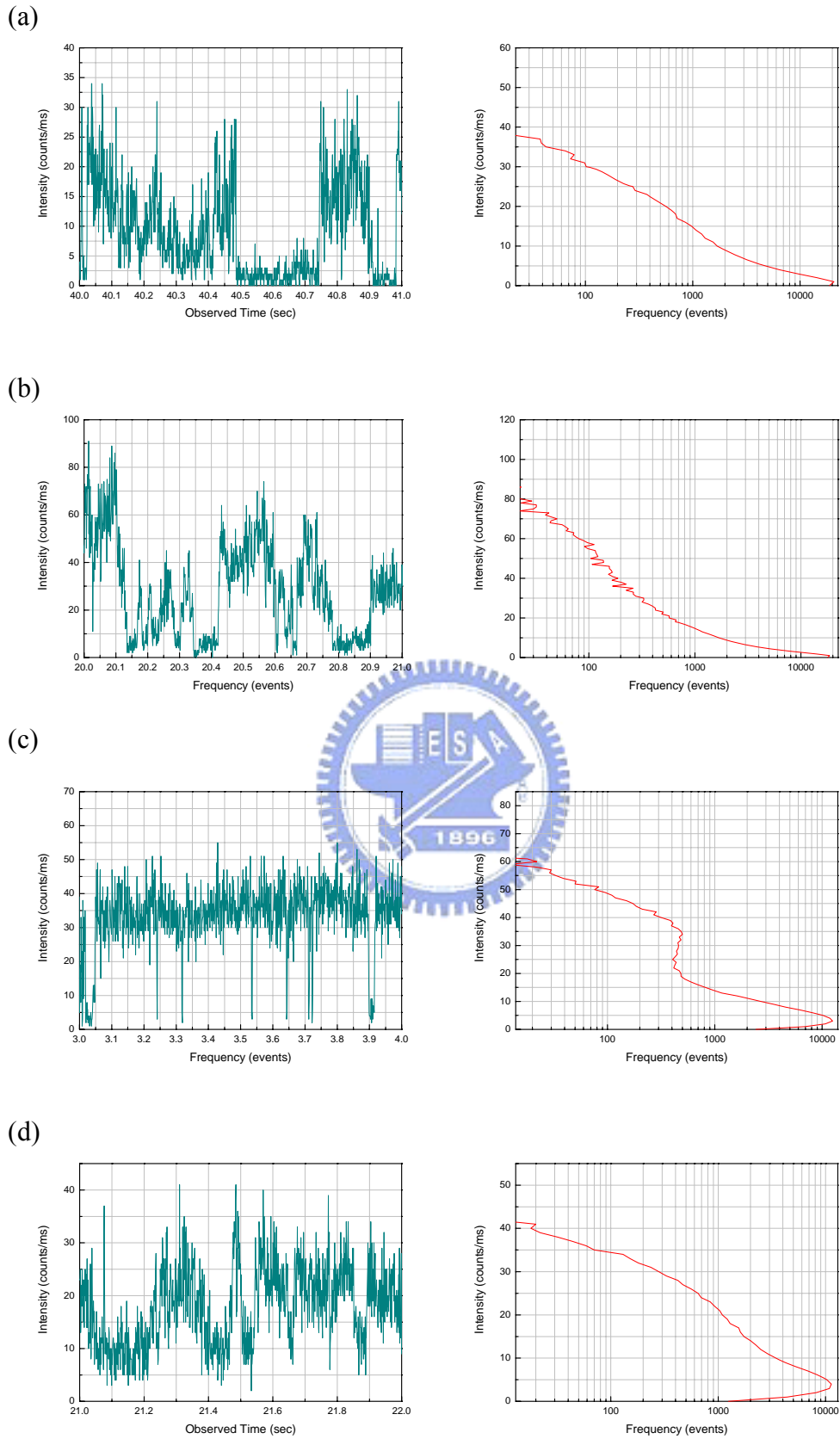
(a)

(b)

Figure 4.5.2 (a) PL and (b) absorption spectra of surface-ligand CdSe/ZnS QDs of 3nm in diameter.
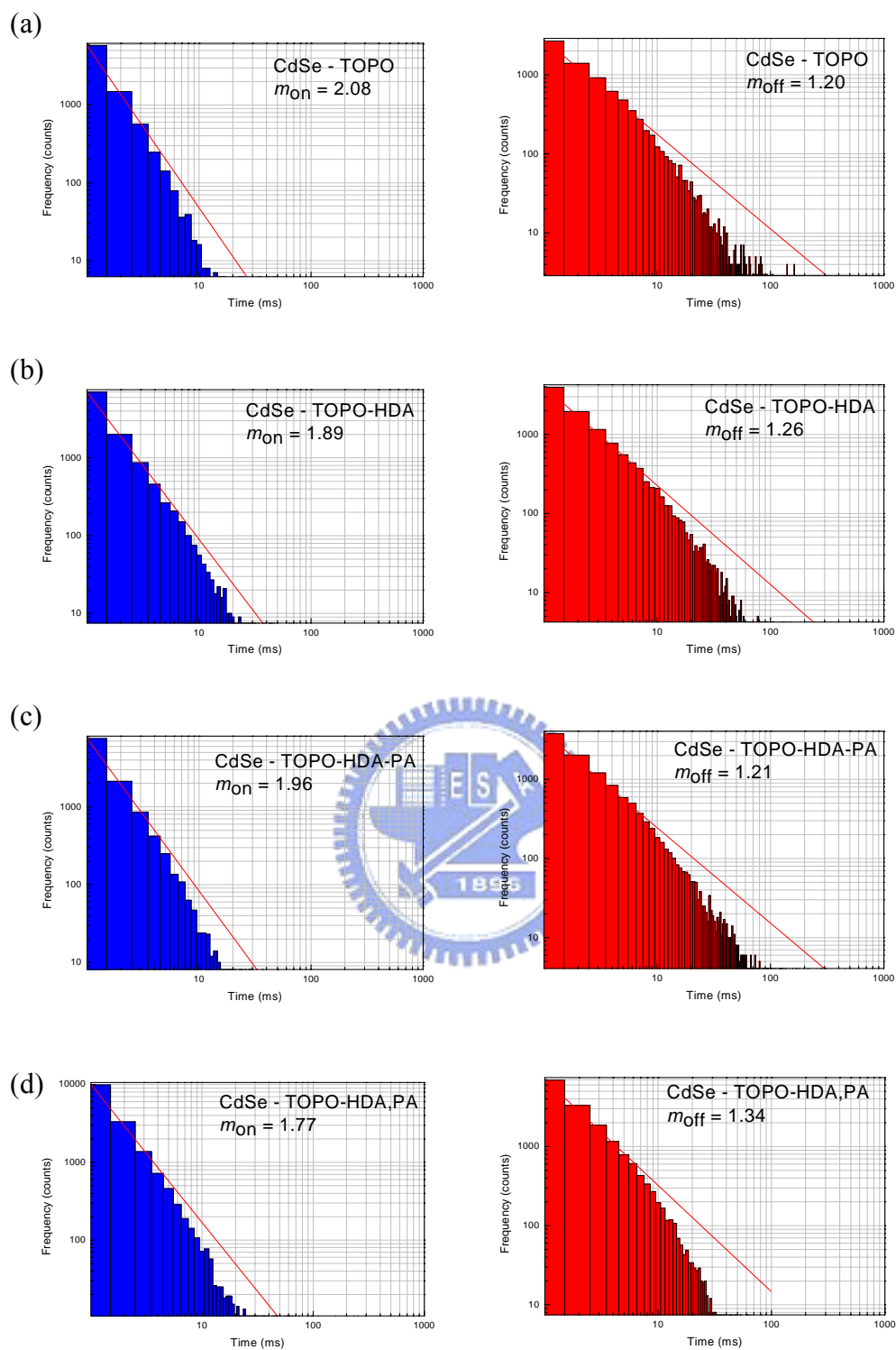
(a)

(b)

(c)

(d)

Figure 4.5.3   Time traces of CdSe nanocrystals with (a) TOPO (b) TOPO-HDA (c)TOPO- HDA-PA (d) TOPO-HDA, PA added at the same time.

(a)

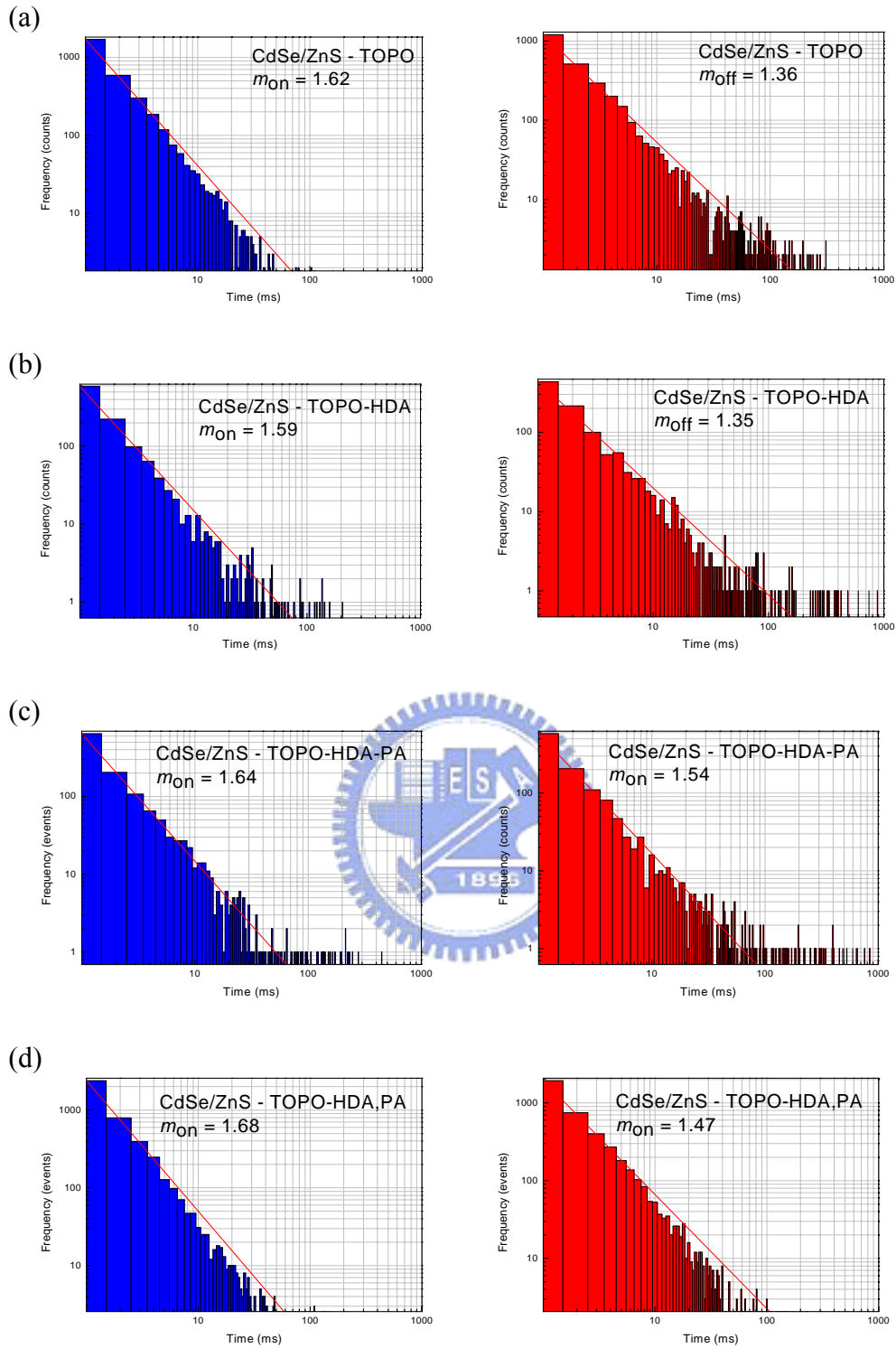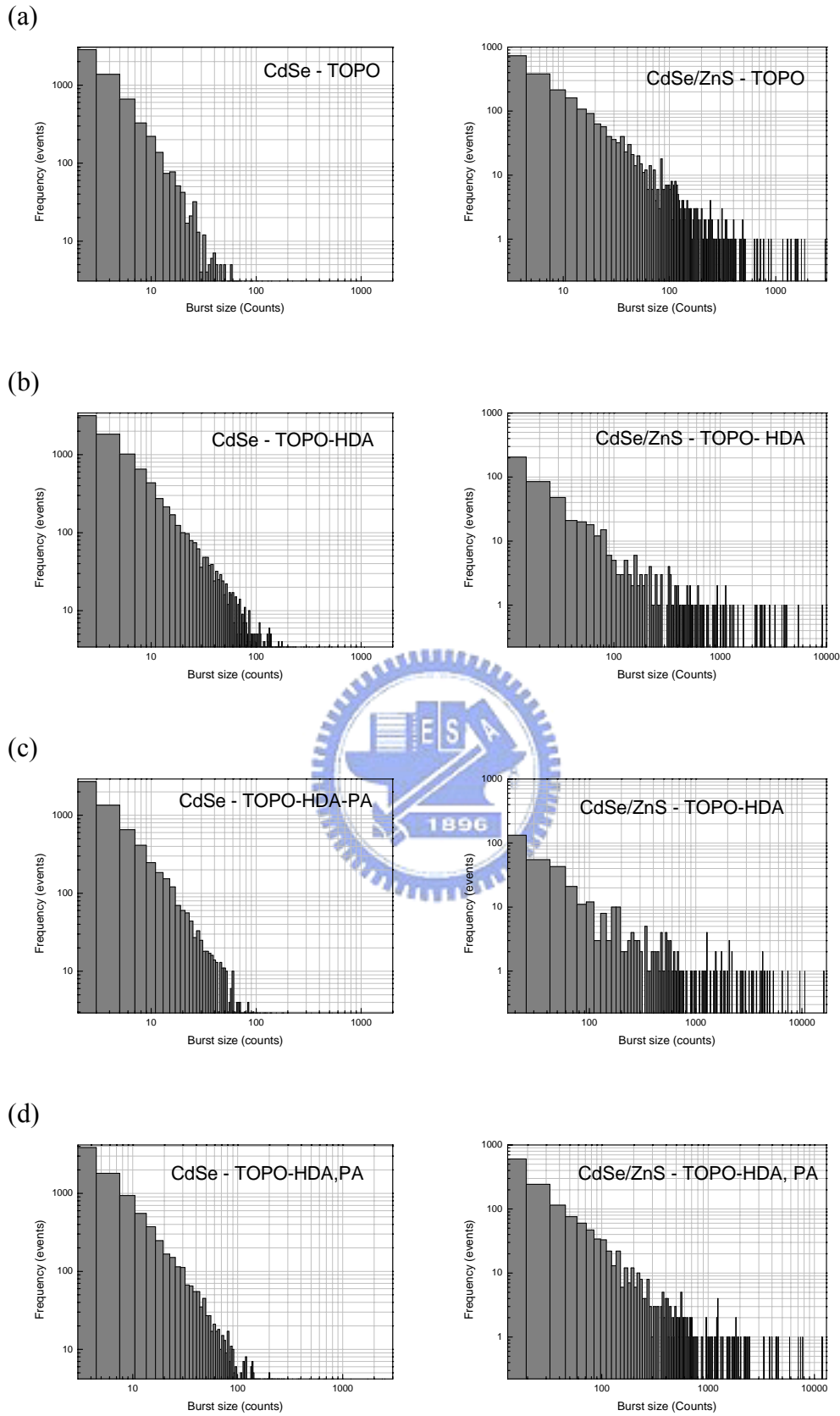(b)

(c)

(d)

Figure 4.5.4   Time traces of CdSe/ZnS QDs with (a) TOPO (b) TOPO-HDA (c)TOPO- HDA-PA (d) TOPO-HDA, PA added at the same time.

Figure 4.5.5   On-time (left) and off-time (right) histogram of single CdSe nanocrystal with (a) TOPO (b) TOPO-HDA (c)TOPO- HDA-PA (d) TOPO-HDA, PA added at same time.

(a)

(b)

(c)

(d)

Figure 4.5.6 The on-time (left) and off-time (right) histogram of single CdSe/ZnS QDs with (a) TOPO (b) TOPO-HDA (c)TOPO- HDA-PA (d) TOPO-HDA, PA added at same time.

(a)

(b)

(c)

(d)

Figure 4.5.7 CdSe (left) and CdSe/ZnS QDs (right) with (a) TOPO (b) TOPO-HDA (c) TOPO-HDA-PA (d) TOPO-HDA, PA added at same time

55

(a)

(b)

(c)

(d)
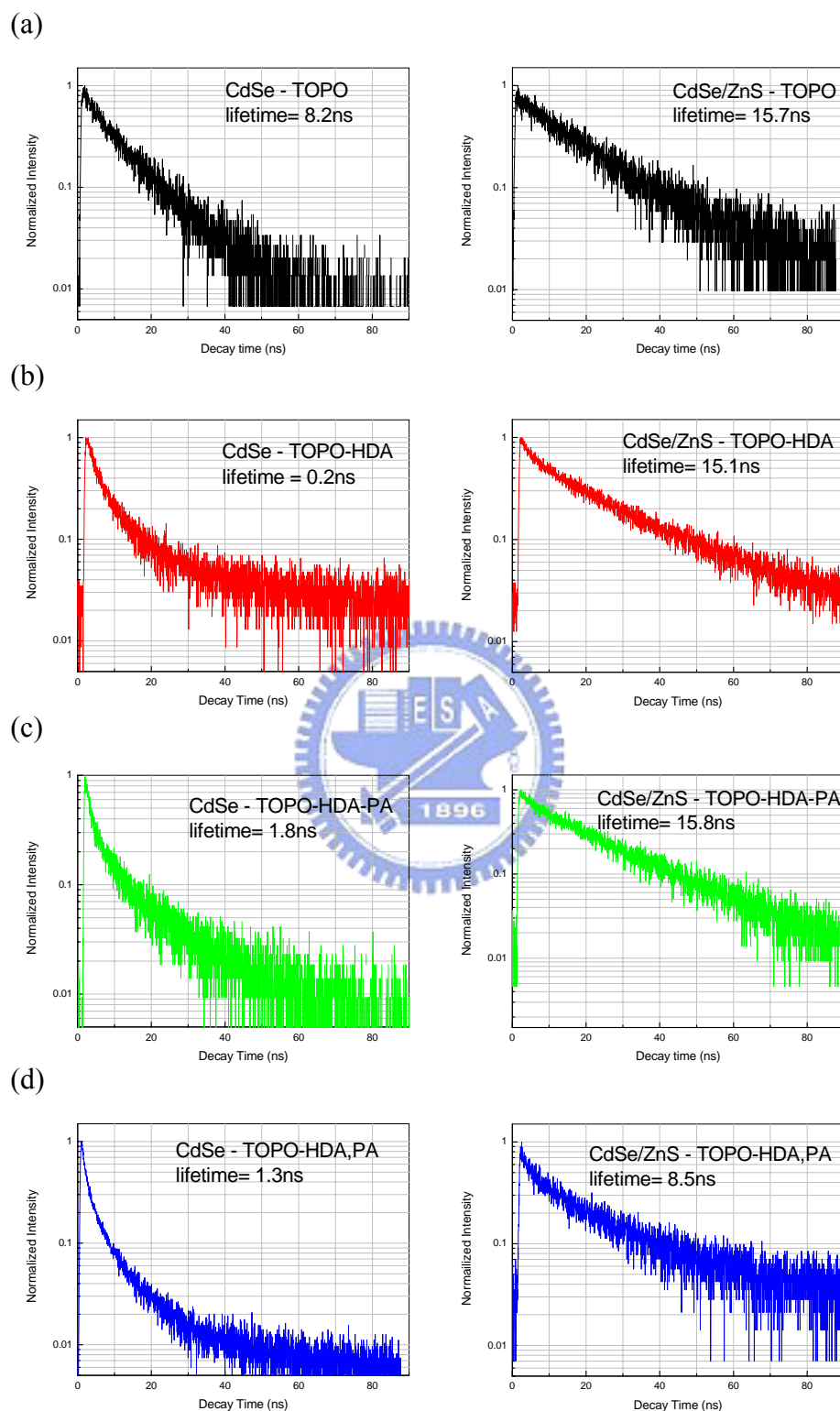
Figure 4.5.8   Decay time profile of CdSe (left) and CdSe/ZnS (right) with ligand conjugation in (a) TOPO (b) TOPO-HDA (c) TOPO-HDA-PA (d) TOPO, then HDA and PA added at the same time

Table 4.1   Sample parameters of the ligand conjugated CdSe and CdSe/ZnS QDs which emit green light.

Sample	Conjugated Ligand	Lifetime (ns)	On-time (ms)	Off-time (ms)	On-time ratio	β	Intensity (Counts/ms)
CdSe	TOPO	8.2	5.2	5.5	0.48	0.8	656
	TOPO-HDA	0.2	7.8	7.2	0.52	0.3	521
	TOPO-HDA-PA	1.8	4.6	3.6	0.56	0.5	552
	TOPO-HDA,PA	1.3	4.6	4.5	0.49	0.5	478
CdSe/ZnS	TOPO	15.7	31.9	16.1	0.65	0.7	2690
	TOPO-HDA	15.1	38.8	12.9	0.75	0.8	7710
	TOPO-HDA-PA	15.8	46.4	11.7	0.80	0.9	9125
	TOPO-HDA,PA	8.5	26.7	10.9	0.71	0.6	3797